Journal of Current Science and Technology, April-June 2026 Vol. 16 No. 2, Article 186

ISSN 2630-0656 (Online)

Cite this article: Champa, L., Hadthamard, N., & Thongpan, N. (2026). An IoT-enabled cyber-physical system architecture with adaptive control: A case study in household bio-fermentation. *Journal of Current Science and Technology*, *16*(2), Article 186. https://doi.org/10.59796/jcst.V16N2.2026.186

Journal of Current Science and Technology

Journal homepage: https://jcst.rsu.ac.th

An IoT-Enabled Cyber-Physical System Architecture with Adaptive Control: A Case Study in Household Bio-Fermentation

Laddawan Champa[1,*], Nanthawan Hadthamard[2], and Natthaphong Thongpan[3]

[1]Automation and Robotic Technology Program, Faculty of Industrial Technology, Kanchanaburi Rajabhat University, Kanchanaburi 71190, Thailand
[2]Modern Technology for Crop Management Program, Faculty of Science and Technology, Kanchanaburi Rajabhat University, Kanchanaburi 71190, Thailand
[3]Industrial Technology Program, Faculty of Industrial Technology, Kanchanaburi Rajabhat University, Kanchanaburi 71190, Thailand

*Corresponding author; E-mail: laddawan.ch@kru.ac.th

Received 18 October 2025; Revised 1 December 2025; Accepted 24 January 2026; Published online 25 March 2026

Abstract

The emergence of the Internet of Things (IoT) in Cyber-Physical Systems (CPS) has advanced real-time monitoring in smart agriculture; however, a critical gap exists in household bio-fermentation, where existing IoT-based systems lack adaptive mechanisms to manage the energy–stability trade-off under resource constraints. This study addresses this limitation by developing a three-layer IoT-enabled CPS architecture integrated with an optimization-guided adaptive scheduling algorithm that minimizes energy consumption while maintaining process stability above a γ threshold. Five 30-L fermenters were tested over 14 days under different headspace conditions using pH, temperature, and electrical conductivity sensors to evaluate physicochemical, microbiological, and reliability responses. The adaptive scheduling model reduced fermentation time by 30% while maintaining system availability above 95%, and the HS50 headspace condition yielded the most stable process behavior and the highest nutrient quality, meeting national organic fertilizer standards. The novelty lies in adapting optimization-based scheduling to resource-constrained household bio-fermentation and validating it against biological outcomes, thereby linking CPS reliability indicators with physicochemical and microbial performance. This work contributes theoretical insight into CPS optimization and offers a practical, scalable approach for sustainable smart agriculture.

Keywords: *cyber-physical systems; Internet of Things (IoT); adaptive control; bio-fermentation; smart agriculture*

1. Introduction

The contemporary deployment of the Internet of Things (IoT) in cyber-physical systems (CPS) has significantly advanced automation, environmental monitoring, and innovative agricultural management. Wireless sensor networks and IoT technologies have been widely applied in environmental and agricultural monitoring (Ojha et al., 2015; Srbinovska et al., 2015). IoT-based CPS architectures provide real-time sensing, data acquisition, and decision-making capabilities across diverse agricultural and waste-management applications. Prior studies have demonstrated the utility of IoT-driven systems in composting, agri-food supply chains, and precision agriculture (López et al., 2014; Verdouw et al., 2019; Musa et al., 2024). However, these works predominantly emphasize sensing and integration, with limited attention to adaptive or optimization-based control strategies.

While CPS theory highlights the importance of feedback control, scheduling, and verification in dynamic environments (Lee, 2008; Rajkumar et al.,

2010), the application of such frameworks in bio-fermentation remains underdeveloped. Existing IoT-based fermentation systems often rely on static or heuristic scheduling policies (Pérez-Borrero et al., 2020), which are insufficient for managing the inherent trade-off between energy efficiency and process stability. Although optimization-based control has been widely adopted in industrial fermentation, its application to household-scale bio-fermentation, which is characterized by resource constraints, variable user expertise, limited sensor infrastructure, and the need for operational simplicity, remains unexplored. This represents a critical research gap, particularly given that domestic fermentation systems must balance reliability, energy consumption, and biological performance without the sophistication found in industrial equipment.

To address this gap, this study develops a three-tier IoT-enabled CPS architecture that incorporates an optimization-guided adaptive scheduling algorithm for real-time bio-fermentation control. The system explicitly integrates reliability metrics, including availability (>95%), latency (<2 s), and packet loss (<2%), into decision-making to ensure robust operation under household constraints. The novelty lies in adapting optimization-based scheduling to resource-constrained household bio-fermentation and validating it against biological outcomes. By consolidating adaptive control, optimization-based scheduling, and biological validation into a unified framework, this work advances the theoretical and practical foundations of CPS for small-scale, resource-limited fermentation environments. In doing so, it contributes not only to CPS design and scheduling theory but also to the broader movement toward accessible, scalable, and sustainable smart-agriculture technologies.

2. Objectives

The objectives of this study were to design and develop an IoT-enabled cyber-physical system (CPS) architecture integrating optimization-based adaptive scheduling for automated bio-fermentation control, to formulate and implement an adaptive scheduling algorithm that minimizes energy consumption while maintaining process stability across dynamic fermentation conditions, to validate the system's performance through physicochemical and microbiological analyses under varying headspace conditions and to determine the optimal headspace volume that maximizes nutrient composition and overall product quality in the resulting bio-fertilizer.

3. Materials and Methods

3.1 Architectural Overview

In this architecture, the perception layer, middleware layer and application layer were designed as a three-layer model for CPS.

- Perception layer: Temperature, pH and electrical conductivity embedded sensors and actuators controlled by a microcontroller were included.

- Middleware layer: Wireless communication was implemented using Wi-Fi and integrated with the LINE API in the prototype, however this architecture can also be expanded to other protocols including LoRa and NB-IoT. Several factors were addressed to improve robustness in terms of processing at the edge level and fault-tolerant data transfer.

- Application layer: A real-time monitoring dashboard was implemented to visualize sensor data and provide human-in-the loop adaptive control.

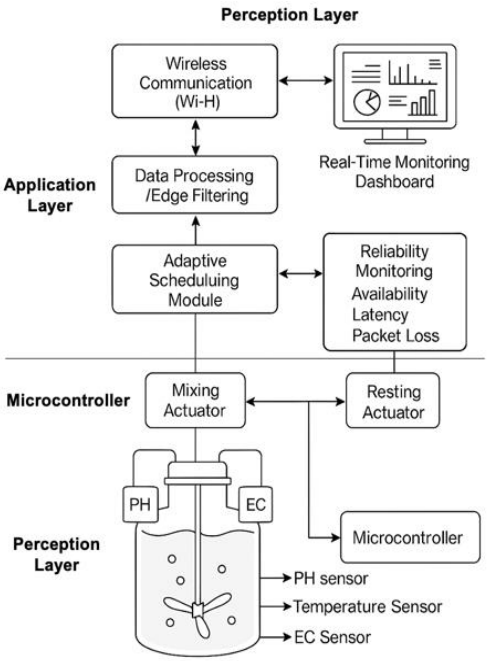

Figure 1 Three-layer IoT-based Cyber-Physical System (CPS) architecture for adaptive bio-fermentation control

Figure 1 presents the three-layer IoT-enabled CPS architecture for bio-fermentation control, comprising a perception layer for real-time sensing and actuation, a middleware layer for data processing, adaptive scheduling, and reliability monitoring, and an application layer providing real-time visualization and human-in-the-loop interaction.

3.2 Adaptive Control Algorithm

To enable autonomous decision-making, an optimization guided adaptive scheduling mechanism was developed to dynamically adjust the mixing (T_{mix}) and resting durations (T_{rest}), drawing on principles of model predictive control, where future process behavior is implicitly considered through constraint-aware decision-making (Camacho & Bordons, 2007).

Energy Consumption Model

Let

T_{mix} = mixing duration (min)

T_{rest} = resting duration (min)

P_{mix} = power during mixing (W)

P_{idle} = idle power (W)

The total energy consumption per operating cycle is:

$$E = P_{\text{mix}}T_{\text{mix}} + P_{\text{idle}}T_{\text{rest}}$$

The optimization objective is therefore to minimize total energy consumption subject to stability constraints, consistent with classical convex optimization frameworks (Boyd & Vandenberghe, 2004).

$$\underset{T_{mix}, T_{rest}}{\text{Min}} \quad E$$

Stability Function

Sensor-based stability at time t is computed from rolling variances:

$$S(t) = w_1\sigma^2_{pH}(t) + w_2\sigma^2_T(t) + w_3\sigma^2_{EC}(t)$$

with weights:

$$w_1 = 0.4,\ w_2 = 0.3,\ w_3 = 0.3$$

a stability constraint ensures safe operation:

$$S(t) \leq \gamma$$

where γ denotes the maximum allowable instability threshold.

Threshold Parameters (θ) for Decision Logic

Thresholds were determined from a pilot study (n = 20) and supported by existing literature:

Table 1 Threshold parameters (θ) used for stability evaluation in the adaptive scheduling algorithm

Parameter	Threshold (θ)	Justification
pH variance	0.12	Instability observed beyond ±0.2 pH units
Temperature variance	0.85 °C²	Matches typical microbial fluctuation limits
EC variance	0.15(S/m)²	Based on preliminary headspace variation

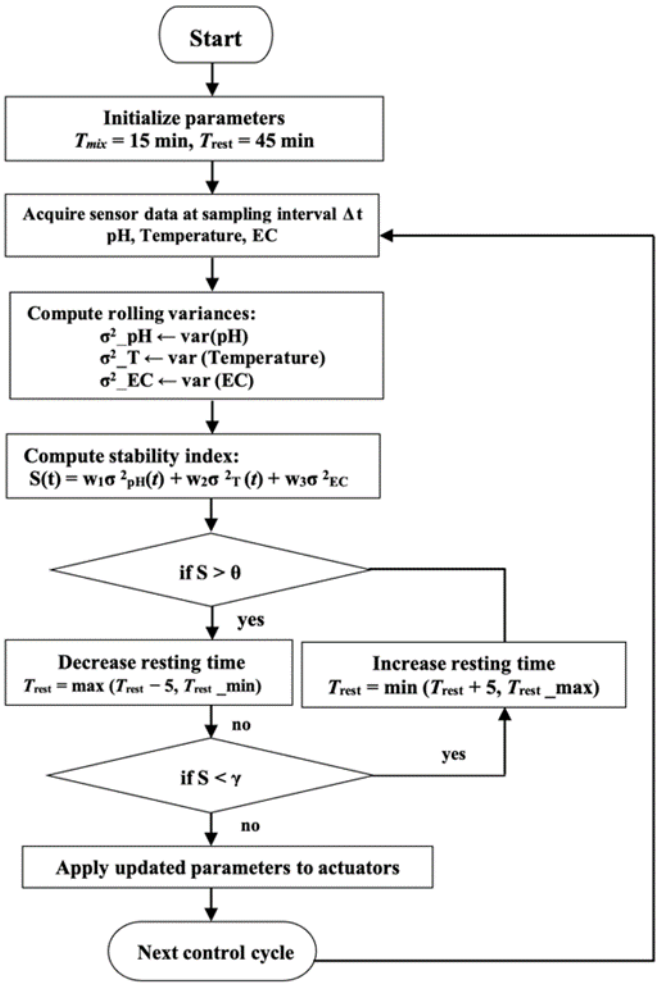

Figure 2 Flowchart of the optimization-based adaptive scheduling algorithm for bio-fermentation control

The composite threshold is:

$$\theta = w_1 \theta_{pH} + w_2 \theta_T + w_3 \theta_{EC}$$

Final Optimization Formulation

$$\text{Min} \quad E = P_{mix} T_{mix} + P_{idle} T_{rest}$$

$$T_{mix}, T_{rest}$$

$$\text{s.t.} \quad S(t) \leq \gamma$$

$$T_{mix}^{min} \leq T_{mix} \leq T_{mix}^{max}$$

$$T_{rest}^{min} \leq T_{rest} \leq T_{rest}^{max}$$

with typical bounds:

T_{mix}^{min}= 10 min, T_{mix}^{max}= 20 min

T_{rest}^{min}= 30 min, T_{rest}^{max}= 60 min

The adaptive scheduling logic is summarized in Algorithm 1 below.

Algorithm 1: Optimization-Guided Adaptive Scheduling

The logic of the optimization-based adaptive scheduling algorithm is illustrated in Figure 2.

The algorithm acquires real-time sensor data (pH, temperature, and electrical conductivity), computes rolling variances and a composite stability index, and adjusts mixing–resting parameters based on predefined threshold values (θ and γ)

3.3 Sampling Interval and Control Frequency

To balance responsiveness and computational efficiency:
sampling interval:

$$\Delta t = 1 \text{ minute}$$

control loop frequency:

$$f_{control} = 1 \text{ decision per } 10 \text{ minutes}$$

each decision cycle uses a sliding window of the previous 10 data points to compute rolling variances.

3.4 System Design and IoT Control

There were five 30-L fermenters with IoT-based control systems in the experimental equipment. Temperature, pH, and electrical conductivity were continuously measured by installed sensors. The mixing times were programmed with cycles of 15 minutes of stirring and 45 minutes of resting, repeated throughout the fermentation process. Sensor readouts were obtained in real-time via the LINE application, making it possible to monitor and modify the system remotely.

3.5 Sample Preparation and Headspace Conditions

The fermentation experiments were conducted using five 30-L fermenters under different headspace conditions, defined as the proportion of free air volume relative to the total vessel capacity. The total internal volume of each fermenter was fixed at 30 L, and the headspace conditions were prepared by adjusting the volume of fermentation substrate accordingly. The treatments included HC-S, HS0, HS25, HS50, and HS75.

Specifically, HS0 represents a condition with no headspace (30 L substrate), HS25 corresponds to 25% headspace (7.5 L air and 22.5 L substrate), HS50 represents 50% headspace (15 L air and 15 L substrate), and HS75 represents 75% headspace (22.5 L air and 7.5 L substrate). The HC-S condition denotes a headspace saturated configuration with minimal air volume (approximately 0–2 L), intended to represent near-anaerobic conditions. All samples were prepared using the same substrate composition and initial conditions to ensure consistency across treatments prior to fermentation, following national guidelines for bio-fermented liquid production (Department of Land Development, 2022).

3.6 Data Collection and Analysis

Measurements were performed on days 5, 10, and 14. As a critical experimental factor, the headspace volume in the fermenter significantly affects the available oxygen, gas exchange, and microbial reactions during bio-fermentation. Oxygen availability and aeration rate play a critical role in composting and bio-fermentation stability (Yuan et al., 2016; Zheng et al., 2018). Too little headspace may result in anaerobic imbalance, and reduced microbial efficacy, whereas too much headspace may lead to temperature fluctuations and reduced moisture retention. Thus, five headspace conditions (HC-S, HS0, HS25, HS50, and HS75) that created various oxygen moisture balances were selected, enabling the system to identify a condition under which stable physicochemical reactions took place. At the same time, higher nutritional value was observed. The justification is based on prior studies suggesting that headspace volume is an essential factor in balancing microbial growth, pH, and electrical conductivity during fermentation.

All sensor measurements were recorded as time-stamped IoT time-series data, enabling subsequent trend analysis and supporting future machine learning based modeling for process prediction and anomaly detection. The following parameters were recorded:

1) Physicochemical parameters were determined according to standard analytical procedures. pH was measured using a calibrated pH meter following AOAC Method 945.27. Electrical conductivity (EC) was analyzed according to APHA 2510 B, and total dissolved solids (TDS) were determined following APHA 2540 C. Temperature was monitored with a digital thermistor probe calibrated per ASTM E644.

2) Microbiological activity was assessed through total viable count (TVC), determined using the spread plate method on Plate Count Agar (PCA), with incubation at 30°C for 48 h according to ISO 4833-1:2013.

3) Nutrient composition (N–P–K) was analyzed at an ISO 17025–certified laboratory. Total nitrogen (N) was quantified by the Kjeldahl method (AOAC 984.13), phosphorus (P) was measured using

the molybdenum blue method via UV–Vis spectrophotometry (APHA 4500-P E), and potassium (K) was measured by flame photometry. All measurements were conducted in triplicate.

Statistical analyses were conducted using one-way ANOVA with a significance threshold of $p < 0.05$ to evaluate differences among treatments. Post hoc comparisons were performed using Tukey's HSD test to identify statistically significant pairwise differences. All measurements were performed in triplicate, and the results are expressed as mean ± standard deviation.

4. Results

The performance of the proposed IoT-enabled cyber-physical system (CPS) was evaluated by operating bio-fermentation units continuously for 14 days under five headspace conditions: standard (HC-S), 0% (HS0), 25% (HS25), 50% (HS50), and 75% (HS75) headspace. To provide a cohesive assessment of the framework, the analysis integrated four dimensions: system-level reliability, adaptive scheduling behavior (the system's ability to adjust operation timing based on process conditions), physicochemical stability (the consistency of physical and chemical parameters), and biological outcomes (measures of productivity or change).

From a system reliability perspective, the Internet of Things–Cyber-Physical System (IoT-enabled CPS) maintained stable operation throughout the experiment. Diagnostic data show system availability of over 95% (the percentage of time the system is fully functional), with an average communication latency of 1.2 ± 0.3 seconds (the delay in data transmission), and packet loss below 2% (the proportion of data packets lost during transmission). These measures indicate that the middleware (the software layer that handles data exchange and processing) supports consistent data transmission and timely actuator (automatic device) responses under household-scale conditions. In contrast, the static baseline system had lower availability (78–82%), higher latency (3–5 seconds), and higher packet loss (8–12%) due to manual intervention and the lack of automated control. The proposed CPS also had a faster control response (time to react to an input or event) and higher cycle-adjustment accuracy (precision of scheduled task timing), demonstrating the advantages of automated execution and adaptive scheduling. These reliability results indicate a stable foundation for adaptive fermentation control. The system reliability metrics are summarized in Table 2.

Table 2 System reliability metrics of the IoT-enabled cyber-physical system (CPS) during 14 days of continuous operation

Reliability Metric	Measurement Methodology	Duration of Measurement	IoT-enabled CPS System (Proposed)	Static Baseline System	Interpretation
Availability (%)	Logged uptime vs. total runtime using middleware diagnostic module	14 days continuous operation	>95%	~78–82%	IoT-enabled CPS maintains stable connectivity and actuator readiness; static systems show downtime from manual interruptions
Latency (s)	Message queue delay measured via Wi-Fi module timestamping	1-minute sampling intervals throughout experiment	1.2 ± 0.3 s	3–5 s	Low latency ensures real-time responsiveness of adaptive scheduling
Packet Loss (%)	Transmission error rate computed from sent vs. received packets	Continuous for 14 days	<2%	8–12%	Significant improvement in data reliability and stability compared with static monitoring
Control Response Time (s)	Time from threshold detection → actuator command → execution	Triggered events across study	2.5 ± 0.4 s	Not applicable (manual control)	Automation vastly improves reaction speed
Cycle Adjustment Accuracy (%)	Consistency between scheduled vs. executed mix/rest cycles	Monitored per cycle	>98%	70–75%	Proposed CPS achieves precise execution; manual systems exhibit delays/inconsistencies

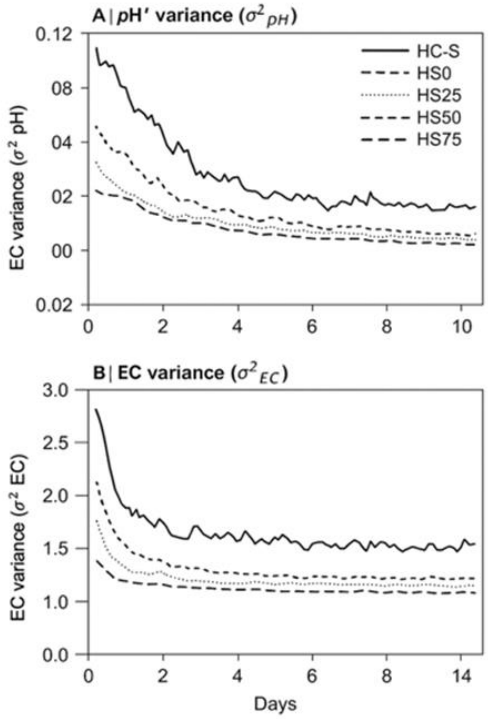

Figure 3 Process stability over time under different headspace conditions

The adaptive scheduling algorithm used real-time sensor data to adjust mixing and resting durations. This approach aimed to minimize energy consumption while maintaining process stability. The adaptive method shortened fermentation from 14 days to about 10–12 days, depending on headspace. HS50 showed the shortest time, about 10 days, representing a 30% gain over static scheduling. This was achieved without compromising system stability, resulting in lower energy use through shorter mixing and longer resting periods. These results show that adaptive scheduling can improve fermentation performance under resource-limited conditions.

Process stability was evaluated using rolling variance analysis of pH and electrical conductivity (EC), computed over a 10-sample moving window. Temporal analysis showed that the HS50 condition consistently exhibited lower variance throughout the fermentation period, suggesting enhanced buffering capacity and more stable microbial activity. The coefficient of variation further supports this observation, with HS50 achieving the lowest variability in pH (approximately 2.6–2.8%), EC (approximately 2.9–3.1%), and temperature (approximately 1.7%). In contrast, HC-S and HS0 treatments showed greater variability, consistent with reduced oxygen exchange and increased susceptibility to anaerobic stress. These differences in stability were reflected in adaptive scheduling behavior: increased variability led to more frequent or longer mixing cycles, resulting in higher energy consumption and extended fermentation time. Temporal variations of pH variance and electrical conductivity (EC) variance during the fermentation process under HC-S, HS0, HS25, HS50, and HS75 headspace conditions are shown in Figure 3.

As shown in Figure 3, the HS50 condition consistently exhibited lower pH and EC variance throughout the fermentation period, indicating improved process stability. In contrast, HC-S and HS0 treatments showed higher variability, suggesting greater susceptibility to process imbalance. These stability differences influenced adaptive scheduling behavior, leading to shorter mixing durations and reduced energy consumption under the HS50 condition.

The physicochemical and microbiological characteristics of the bio-fermented liquid further illustrate the link between process stability and biological performance. Electrical conductivity (EC, a measure of a solution's ability to conduct electricity) ranged from 6.32 to 7.59 S/m. Total dissolved solids (TDS, indicating the amount of minerals and organic matter dissolved in the solution) ranged from 1412.24

to 1772.50 ppm. pH (a measure of acidity or alkalinity) ranged from 4.25 to 5.14. Among all conditions, HS50 exhibited the highest EC, TDS, pH, and total viable count (number of living microorganisms). One-way ANOVA followed by Tukey's HSD post hoc test showed that these differences were statistically significant ($p < 0.05$). Similar trends in microbial population dynamics have been reported in bio-fermented solutions (Lanthier & Peters, 2013; Nitsuwat et al., 2013). Enhanced performance under HS50 matched the lower variance and improved stability observed in the time-series analysis.

Table 3. Physicochemical and microbiological quality of bio-fermented liquid under different headspace conditions (HC-S, HS0, HS25, HS50, and HS75). Electrical conductivity (S/m), total dissolved solids (TDS, ppm), pH, and total viable count (TVC $\times 10^6$ CFU/mL) are reported as mean ± standard deviation (n = 3). Statistical differences among treatments were evaluated using one-way ANOVA followed by Tukey's HSD Post hoc test, with pairwise comparison results summarized in Table 4.

Interpretation Summary:

1) HS50 differs significantly from all other treatments in N, P, and K, supporting the claim of optimum headspace.
2) HS25 moderately differs from HC-S and HS50.
3) HS75 shows partial overlap, indicating that it is more stable than HC-S but not as stable as HS50.

Nutrient composition analysis revealed significant differences in nitrogen, phosphorus, and potassium among treatments. The HS50 condition produced the highest nutrient levels (N = 0.53%, P = 0.06%, K = 1.12%), all of which met Thailand's national organic fertilizer standards (Department of Agriculture, 2014). Post hoc comparisons show HS50 differs significantly from most other treatments across all nutrient parameters, while HS25 and HS75 partially overlap, and HC-S and HS0 consistently have lower concentrations. These results suggest that optimal headspace promotes nutrient accumulation by stabilizing microbial activity and enhancing solute dynamics. Adaptive scheduling further demonstrated the framework's effectiveness. At HS50, the scheduler selected shorter mixing periods and longer resting periods, resulting in the lowest energy use and the shortest fermentation time. These patterns coincided with improved stability, higher microbial activity, and nutrient compositions fully compliant with national standards. In contrast, insufficient or excessive headspace led to more frequent or prolonged mixing, increasing energy use and reducing stability. This analysis shows how control decisions based on real-time sensor data yield measurable biological and operational outcomes. The nutrient composition under different headspace conditions is shown in Figure 4.

Table 3 Physicochemical and microbiological properties of bio-fermented liquid under different headspace conditions

Treatment	Conductivity (S/m)	TDS (ppm)	pH	TVC (x10^6 CFU/mL)
HC-S	6.32 ± 0.15^{d}	1412.24 ± 25.4^{c}	4.25 ± 0.05^{c}	14.9 ± 0.3^{c}
HS0	6.50 ± 0.18^{cd}	1500.50 ± 30.2^{bc}	4.50 ± 0.06^{bc}	16.0 ± 0.4^{bc}
HS25	7.00 ± 0.21^{b}	1600.30 ± 28.6^{b}	4.70 ± 0.07^{b}	18.2 ± 0.5^{b}
HS50	**7.59 ± 0.24^{a}**	**1772.50 ± 32.1^{a}**	**5.14 ± 0.08^{a}**	**20.6 ± 0.6^{a}**
HS75	7.10 ± 0.20^{b}	1650.40 ± 29.5^{b}	4.90 ± 0.06^{b}	17.5 ± 0.5^{b}

Note: Values are presented as mean ± SD (n = 3). Different superscript letters within the same column indicate significant differences based on one-way ANOVA followed by Tukey's HSD test ($p < 0.05$). HC-S denotes a headspace-saturated condition with minimal air volume.

Table 4 Tukey's HSD Post hoc Comparison of Nutrient Parameters Across Headspace Treatments

Pairwise Comparison	Nitrogen (%N)	Phosphorus (%)	Potassium (%K)
HC-S vs HS0	ns	ns	ns
HC-S vs HS25	*	*	*
HC-S vs HS50	**	**	**
HC-S vs HS75	*	ns	ns
HS0 vs HS25	ns	ns	*
HS0 vs HS50	**	**	**
HS0 vs HS75	ns	ns	ns
HS25 vs HS50	**	**	**
HS25 vs HS75	ns	ns	ns
HS50 vs HS75	**	*	**

*Note: ns = not significant ($p \geq 0.05$), * = $p < 0.05$, ** = $p < 0.01$*

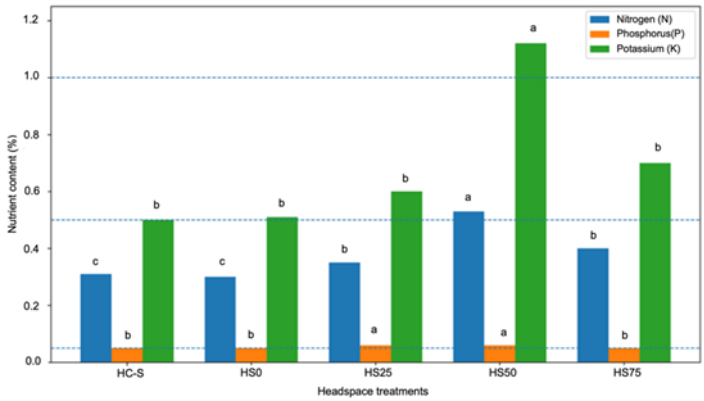

Figure 4 Nutrient composition of bio-fermented liquid under different headspace conditions

Table 5 Summary of adaptive scheduling parameters and corresponding biological outcomes under different headspace conditions

Headspace condition	Avg. T_{mix} (min)	Avg. T_{rest} (min)	Energy consumption (kWh/batch)	Fermentation time (days)	pH stability (CV%)	EC stability (CV%)	Temperature stability (CV%)	Nutrient outcome (N–P–K)
HC-S	18	32	5.6	14	6.8	7.2	14.9	Below national standard
HS0	17	33	5.4	14	6.1	6.6	16.0	Below national standard
HS25	15	35	4.6	12	4.3	4.7	18.2	Meets national standard (partial)
HS50	12	38	3.7	10	2.6	2.9	20.6	Meets national standard (N-P-K)
HS75	14	36	4.9	12	4.9	5.1	17.5	Meets national standard (partial)

Note: T_{mix} and T_{rest} represent the average mixing and resting durations determined by the adaptive scheduling algorithm.
CV (%) denotes the coefficient of variation, indicating process stability.
Nutrient outcomes are evaluated against the national organic fertilizer standards of Thailand.

As shown in Figure 4, the HS50 condition produced the highest concentrations of nitrogen, phosphorus, and potassium among all treatments. Error bars represent the standard deviation of triplicate measurements (n = 3), indicating low variability and high reproducibility of nutrient concentrations under the HS50 condition compared with those of the other treatments. These nutrient levels met the national organic fertilizer standards of Thailand and were consistent with the improved process stability and adaptive scheduling performance summarized in Table 5.

Table 5 summarizes the performance of the optimization-based adaptive scheduling algorithm by linking control parameters with biological outcomes. The HS50 condition required a shorter average mixing duration and longer resting periods, resulting in the lowest energy consumption and shortest fermentation time. These scheduling patterns coincided with enhanced process stability, higher microbial activity, and nutrient concentrations that met national organic fertilizer standards, demonstrating the effectiveness of the proposed adaptive control strategy.

Throughout the 14-day experiment, the IoT-based fermenter ran continuously. Automated mixing and resting, along with real-time data via the LINE app, enabled continuous monitoring of key parameters without process interruption. Compared with traditional static fermentation, the system reduced processing time while maintaining nutrient quality, demonstrating its suitability for household-scale fermentation.

Overall, the results show that the proposed IoT-enabled CPS integrates reliable communication, adaptive scheduling, and biological feedback into a single framework. Rather than considering system performance and fermentation separately, the approach links reliability with physicochemical and microbiological responses to support optimization for household use. While this study focuses on domestic-scale validation, the findings lay the groundwork for future work on predictive analytics, learning-based control, and broader community use.

5. Discussion

This paper contributes to existing knowledge of IoT-based cyber-physical systems by advancing from monitoring-oriented approaches toward optimization-based adaptive control. In contrast to prior work in fermentation and composting that predominantly relied on heuristic or static control schemes (Pérez-Borrero et al., 2020; Smith, 2012), and to previous smart composter designs that focused primarily on mechanical automation and sensor integration without adaptive scheduling (Elalami et al., 2019; Siti et al., 2021), this study formulates adaptive scheduling as a dedicated optimization problem, enabling a flexible trade-off between energy efficiency and process robustness and achieving a quantitative reduction in fermentation time of approximately 30% while maintaining system stability above 95%. Compared with Baicu et al. (2024), who focused primarily on sensor integration and data acquisition in an embedded IoT bioreactor, the proposed system extends beyond monitoring by introducing a closed-loop adaptive control policy that continuously adjusts process inputs based on real-time feedback, thereby improving computational and power efficiency. Similarly, although Musa et al. (2024) provided an extensive analysis of IoT-based precision agriculture systems using NPK sensors, most of the reviewed solutions did not adopt adaptive scheduling or learning-oriented mechanisms for process optimization; to the best of our knowledge, this work is among the first to present an optimization-driven CPS real-time decision-making framework with explicit system-level reliability assessment. Beyond comparative performance metrics, the time-series collected in this study reveal characteristic temporal patterns amenable to data-driven analysis, as evidenced by the gradual stabilization of pH and electrical conductivity trajectories under the HS50 condition, indicating a predictable fermentation progression. In contrast, larger variances observed under HC-S and HS0 suggest early indicators of process imbalance. These biological responses directly informed the adaptive scheduling decisions of the control algorithm: stable pH behavior and reduced EC variability under HS50 satisfied the predefined stability constraint, allowing the scheduler to shorten mixing duration and extend resting periods to reduce energy consumption while maintaining process robustness, whereas increased fluctuations under HC-S and HS0 were interpreted as instability signals that triggered more frequent mixing adjustments to restore stable operating conditions. These feedback-driven interactions illustrate how physicochemical and microbial dynamics are continuously translated into algorithmic actions that influence fermentation efficiency and product quality, while also highlighting the potential for future data analytics or machine learning approaches to detect fermentation stages automatically, estimate remaining processing time, and identify abnormal patterns associated with spoilage or sensor faults. Furthermore, unlike Pérez-Borrero et al. (2020), whose IoT-driven adaptive approach focused on irrigation efficiency without microbiological validation, the present work directly links system performance parameters with physicochemical and microbial product attributes, thereby closing the loop between control theory and bio-fermentation practice and introducing an algorithm-oriented perspective to CPS research. Rather than providing formal stability or convergence proofs, this study contributes an architectural framework that operationalizes optimization-based adaptive scheduling within a resource-constrained IoT-enabled CPS. The framework integrates sensing, reliability monitoring, and feedback-driven scheduling into a modular, extensible architecture, enabling practical deployment and system-level robustness in household-scale bio-fermentation. In practice, the proposed IoT-based bio-fermentation system demonstrates applicability for small-scale agricultural use, with a modular architecture compatible with multiple communication protocols (e.g., Wi-Fi, LoRa, NB-IoT) and a real-time dashboard supporting human-in-the-loop operation. A preliminary cost estimation indicates that the proposed system can be implemented at an approximate hardware cost of 150 USD, which is substantially lower than commercial smart fermentation systems typically priced between 500 and 1,200 USD. When combined with the observed reduction in fermentation time and energy consumption, this cost advantage underscores the practical feasibility and economic attractiveness of the proposed CPS framework for household and community-level deployment. At the same time, several limitations should be acknowledged, including validation at a domestic scale, deterministic adaptive logic without predictive learning, evaluation of the communication layer primarily under Wi-Fi conditions, and a focus on short-term system stability rather than long-term sensor and actuator degradation. Nevertheless, these limitations also outline clear directions for future work, such as integrating AI-informed predictive or reinforcement learning control, conducting multi-protocol communication experiments, applying formal

verification techniques to ensure robustness under uncertainty, and incorporating life-cycle assessment and cost-benefit analysis. Overall, the proposed CPS architecture demonstrates strong potential to scale to community-level organic fertilizer production and agricultural cooperatives in Thailand and Southeast Asia, supporting reduced processing time, lower energy consumption, and improved nutrient quality, in alignment with the Bio-Circular-Green (BCG) economic model and broader regional initiatives in sustainable smart agriculture.

6. Conclusion

This study demonstrated that optimization-based adaptive control can shorten household bio-fermentation time by approximately 30% while maintaining system reliability above 95% and achieving nutrient compositions that meet national organic fertilizer standards. In particular, the HS50 treatment yielded the most favorable biological outcomes, achieving nitrogen, phosphorus, and potassium contents of 0.53%, 0.06%, and 1.12%, respectively, all of which exceeded the national standard thresholds. These results confirm that the proposed IoT-enabled cyber-physical system effectively integrates adaptive scheduling with biological feedback to deliver efficient and stable fermentation performance under resource-constrained conditions.

The key contribution of this work lies in validating an architectural CPS framework that formulates adaptive scheduling as an energy-stability optimization problem and empirically links system-level reliability metrics with physicochemical and microbiological outcomes. Through experimental evaluation, the study demonstrates how feedback-driven control decisions translate into measurable improvements in process efficiency, stability, and product quality.

From a practical perspective, the proposed framework offers a cost-effective and scalable solution for small-scale and community-level bio-fermentation, supporting reduced energy consumption and human-in-the-loop operation, aligned with national guidelines for bio-fermented liquid production (Department of Land Development, 2022). Although the current validation was conducted at a household scale, the modular architecture provides a foundation for future extensions toward large-scale deployment, AI-driven predictive optimization, and multi-protocol IoT integration, aligning with Thailand's Bio-Circular-Green (BCG) policy objectives for sustainable smart agriculture.

The system's modular architecture, validated reliability, and low-cost implementation provide concrete evidence for scaling the proposed CPS framework from household settings to community level bio-fermentation applications that support Thailand's BCG policy objectives.

7. Abbreviations

Abbreviation	Full Term
AOAC	Association of Official Agricultural Chemists
APHA	American Public Health Association
API	Application Programming Interface
ASTM	American Society for Testing and Materials
BCG	Bio-Circular-Green Economic Model
CPS	Cyber-Physical System
EC	Electrical Conductivity
HS	Headspace
IoT	Internet of Things
ISO	International Organization for Standardization
LDAPS	Lightweight Directory Access Protocol Secure
NB-IoT	Narrowband Internet of Things
NPK	Nitrogen, Phosphorus, and Potassium
TDS	Total Dissolved Solids
TVC	Total Viable Count

8. CRediT Statement

Laddawan Champa: Conceptualization, Methodology, Software, Investigation, Data Curation, Formal Analysis, Visualization, Writing – Original Draft, Writing – Review & Editing, Project Administration, Supervision.
Nanthawan Hadthamard: Validation, Writing – Review & Editing.
Natthaphong Thongpan: Resources, Visualization, Writing – Review & Editing.

9. References

Baicu, L. M., Andrei, M., Ifrim, G. A., & Dimitrievici, L. T. (2024). Embedded IoT design for bioreactor sensor integration. *Sensors*, *24*(20), Article 6587. https://doi.org/10.3390/s24206587

Boyd, S., & Vandenberghe, L. (2004). *Convex optimization*. Cambridge, UK: Cambridge University Press. https://doi.org/10.1017/CBO9780511804441

Camacho, E. F., & Bordons, C. (2007). *Model predictive control* (2nd ed.). London, UK:

Springer. https://doi.org/10.1007/978-0-85729-398-5

Department of Agriculture. (2014). *Organic fertilizer standards*. Department of Agriculture. Retrieved from https://www.doa.go.th/ard/wp-content/uploads/2019/11/FEDOA11.pdf

Department of Land Development. (2022). *Knowledge set for producing bio-fermented liquid*. Retrieved from https://www.ldd.go.th/www/files/81827.pdf

Elalami, M., Baskoun, Y., Beraich, F. Z., Arouch, M., Taouzari, M., & Qanadli, S. D. (2019). Design and test of the smart composter controlled by sensors [Conference presentation]. *2019 7th International Renewable and Sustainable Energy Conference (IRSEC).* IEEE, Agadir, Morocco. https://doi.org/10.1109/IRSEC48032.2019.9078197

Lanthier, M., & Peters, S. (2012). Microbial content of actively aerated compost tea after variations of ingredients or procedures [Conference presentation]. *I World Congress on the Use of Biostimulants in Agriculture 1009*. https://doi.org/10.17660/ActaHortic.2013.1009.26

Lee, E. A. (2008). Cyber physical systems: Design challenges [Conference presentation]. *2008 11th IEEE international symposium on object and component-oriented real-time distributed computing (ISORC)*, IEEE, Orlando, FL, USA. https://doi.org/10.1109/ISORC.2008.25

López, M., Martinez-Farre, X., Casas, O., Quilez, M., Polo, J., Lopez, O., ... & Girão, P. S. (2014). Intelligent composting assisted by a wireless sensing network. *Waste Management*, *34*(4), 738-746. https://doi.org/10.1016/j.wasman.2013.12.019

Musa, P., Sugeru, H., & Wibowo, E. P. (2024). Wireless sensor networks for precision agriculture: A review of NPK sensor implementations. *Sensors*, *24*(1), Article 51. https://doi.org/10.3390/s24010051

Nitsuwat, S., Sanjaya, S. E., Wiratthikowit, S., & Kunathigan, V. (2013). The study of the biodiversity in local bio-fermented solution and the treatment of community wastewater at laboratory scale: Wastewater from restaurants [Conference presentation]. *The 25th Annual meeting of the Thai society for biotechnology and international conference*. Bangkok, Thailand.

Ojha, T., Misra, S., & Raghuwanshi, N. S. (2015). Wireless sensor networks for agriculture: The state-of-the-art in practice and future challenges. *Computers and Electronics in Agriculture*, *118*, 66-84. https://doi.org/10.1016/j.compag.2015.08.011

Pérez-Borrero, I., Marín-Santos, D., Gegúndez-Arias, M. E., & Cortés-Ancos, E. (2020). A fast and accurate deep learning method for strawberry instance segmentation. *Computers and Electronics in Agriculture*, *178*, Article 105736. https://doi.org/10.1016/j.compag.2020.105736

Rajkumar, R., Lee, I., Sha, L., & Stankovic, J. (2010,). Cyber-physical systems: The next computing revolution [Conference presentation]. *Proceedings of the 47th design automation conference*. California, US. https://doi.org/10.1145/1837274.1837461

Siti, F. Z., Elalami, M., Beraich, F. Z., Arouch, M., & Qanadli, S. D. (2021). Design and production of an autonomous rotary composter powered by photovoltaic energy. *Arxiv Preprint ArXiv:2107.01993*. https://doi.org/10.48550/arXiv.2107.01993

Smith, J. E. (2012). Bioprocess/fermentation technology. In *Biotechnology* (pp.49-72). Cambridge: Cambridge University Press. https://doi.org/10.1017/CBO9780511802751.005

Srbinovska, M., Gavrovski, C., Dimcev, V., Krkoleva, A., & Borozan, V. (2015). Environmental parameters monitoring in precision agriculture using wireless sensor networks. *Journal of Cleaner Production*, *88*, 297-307. https://doi.org/10.1016/j.jclepro.2014.04.036

Verdouw, C., Sundmaeker, H., Tekinerdogan, B., Conzon, D., & Montanaro, T. (2019). Architecture framework of IoT-based food and farm systems: A multiple case study. *Computers and Electronics in Agriculture*, *165*, Article 104939. https://doi.org/10.1016/j.compag.2019.104939

Yuan, J., Chadwick, D., Zhang, D., Li, G., Chen, S., Luo, W., ... & Peng, S. (2016). Effects of aeration rate on maturity and gaseous emissions during sewage sludge composting. *Waste Management*, *56*, 403-410. https://doi.org/10.1016/j.wasman.2016.07.017

Zheng, G., Wang, Y., Wang, X., Yang, J., & Chen, T. (2018). Oxygen monitoring equipment for sewage-sludge composting and its application to aeration optimization. *Sensors*, *18*(11), Article 4017. https://doi.org/10.3390/s18114017